Supplementary material

RAP1-mediated MEK-ERK pathway defects in Kabuki syndrome

Nina Bögershausen[1,2,3*], I-Chun Tsai[4*], Esther Pohl[1,2,3], Pelin Özlem Simsek Kiper[5], Filippo Beleggia[1,2,3], E. Ferda Percin[6], Katharina Keupp[1,2,3], Angela Matchan[7], Esther Milz[1,2,3], Yasemin Alanay[5,8], Hülya Kayserili[9], Yicheng Liu[1,2,3], Siddharth Banka[10], Andrea Kranz[11], Martin Zenker[12], Dagmar Wieczorek[13], Nursel Elcioglu[14], Paolo Prontera[15], Stanislas Lyonnet[16], Thomas Meitinger[17], A. Francis Stewart[11], Dian Donnai[10], Tim M. Strom[17,18], Koray Boduroglu[5], Gökhan Yigit[1,2,3], Yun Li[1,2,3], Nicholas Katsanis[4,†], and Bernd Wollnik[1,2,3,†]

Content:

- Supplementary Figure 1: Novel variants on chromosome 1 showing Mendelian violation.
- Supplementary Figure 2: Modelling and functional consequences of the p.R163T RAP1A mutation.
- Supplementary Figure 3: Kabuki genes control proper jaw layout during early zebrafish development.
- Supplementary Figure 4: Cytoskeleton alterations of *rap1* morphants and RAP1A^{R163T} fibroblasts.
- Supplementary Figure 5: Rap1 interacts genetically with kmt2d.
- Supplementary Figure 6: The ASCOM complex can be found at the *RAP1B* promoter.
- Supplementary Figure 7: Densitometric measurements of pMEK and pERK in patient cells and MEFs.
- Supplementary Figure 8: Rap1-raf1-mediated MEK-ERK pathway is predominant in early zebrafish embryos.

- Supplementary Table 1: Exome variants detected in the *RAP1B* patient.
- Supplementary Table 2: Comparison of clinical signs of related syndromes.
- Supplementary Table 3: Complete list of primer, morpholino, and CRISPR target sequences used for the study.

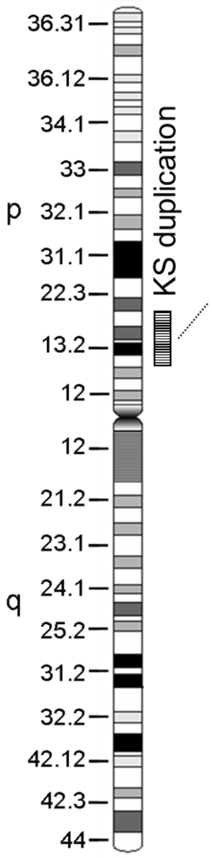

Gene	Chr1	Variant	Depth	Prediction
GABRD	p36.33	c.1117G>A; p.Glu373Lys	47	benign* neutral**
EPHA8	p36.12	c.376T>G; p.Tyr126Asp	36	probably damaging* deleterious**
PABPC4	p34.3	c.1672C>T; p.Pro558Ser	35	benign* neutral**
TCEANC2	p32.3	c.419C>T; p.Ser140Leu	50	benign* neutral**
RAP1A	**p13.2**	**c.488G>C;** **p.Arg163Thr**	**85**	**possibly damaging*** **deleterious****
PPM1J	p13.2	c.1218+5G>A	46	no effect***
CGN	q21.3	c.466A>C; p.Met156Leu	68	benign* neutral**
TCHH	q21.3	c.1447_1449delGAG; p.Glu483del	77	neutral**
LCE2B	q21.3	c.236G>A; p.Arg79His	90	benign* neutral**
ATP1A4	q23.2	c.712G>C; p.Asp238His	92	benign* deleterious**
TBX19	q24.2	c.724C>T; p.His242Tyr	19	probably damaging* neutral**
DTL	q32.3	c.1421C>G; p.Ala474Gly	58	benign* neutral**

Supplementary Figure 1: Novel variants on chromosome 1 showing Mendelian violation. Of 12 novel homozygous variants showing Mendelian violation on chromosome 1, only the *RAP1A* gene lies within the region of the published KS duplication (striped bar; 22). Functional prediction performed with PolyPhen2* and for single nucleotide variants, PROVEAN** for single nucleotide variants and small indels, and BDGP splice site prediction*** for putative splice site variants.

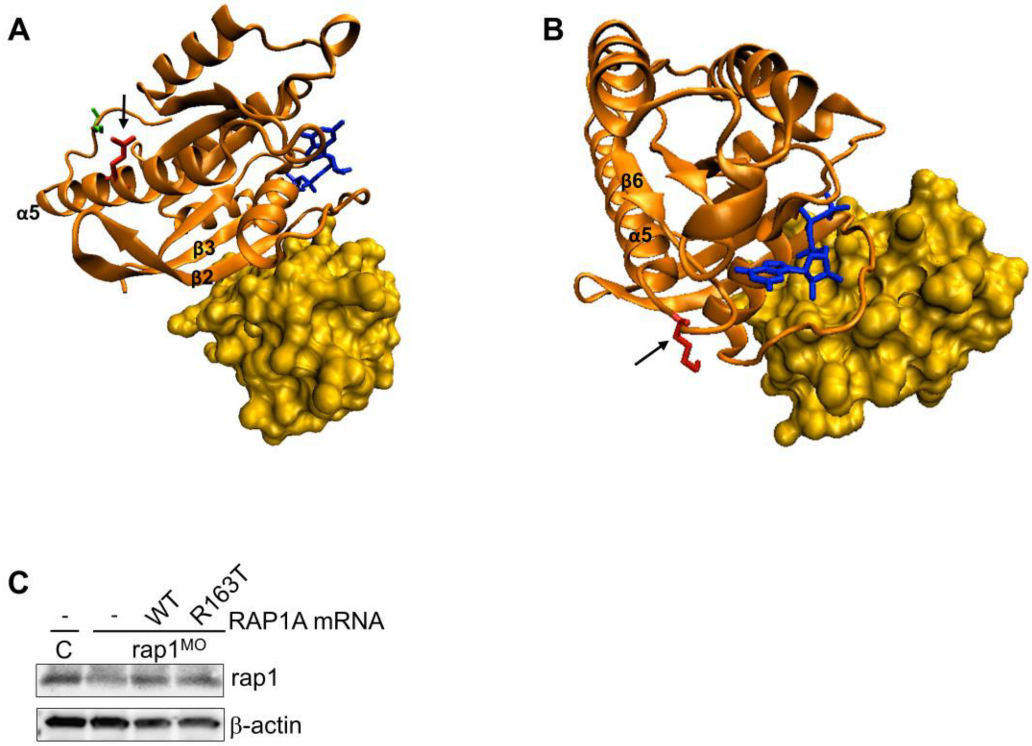

Supplementary Figure 2: Modelling and functional consequences of the RAP1A/B mutations. A, A model of the full length RAP1A protein based on the crystal structure of RAP1A in complex with RAF1 (1C1Y). Orange = RAP1A, yellow = RAF1, blue = GTP, red = mutated amino acids, green = phosphorylation site. Arginine 163 (red, arrow), on the alpha helix 5, is located close to the phosphorylation site at serine 180 and it is not in the vicinity of the binding sites for GTP or RAF1. **B,** Model of the full length RAP1B protein based on the crystal structure of RAP1A in complex with RAF1 (1C1Y). Orange = RAP1B, yellow = RAF1, blue = GTP, red = mutated amino acids. Lysine 151 (red, arrow), on the loop between the beta sheet 6 and the alpha helix 5, is located close to the GTP binding side, but does not directly face or interact with GTP. **C,** Western blot shows the rap1 protein abundance in zebrafish embryos. Human wild-type and mutant protein were expressed at equal levels in embryos injected with *RAP1A* mRNAs (n = 15).

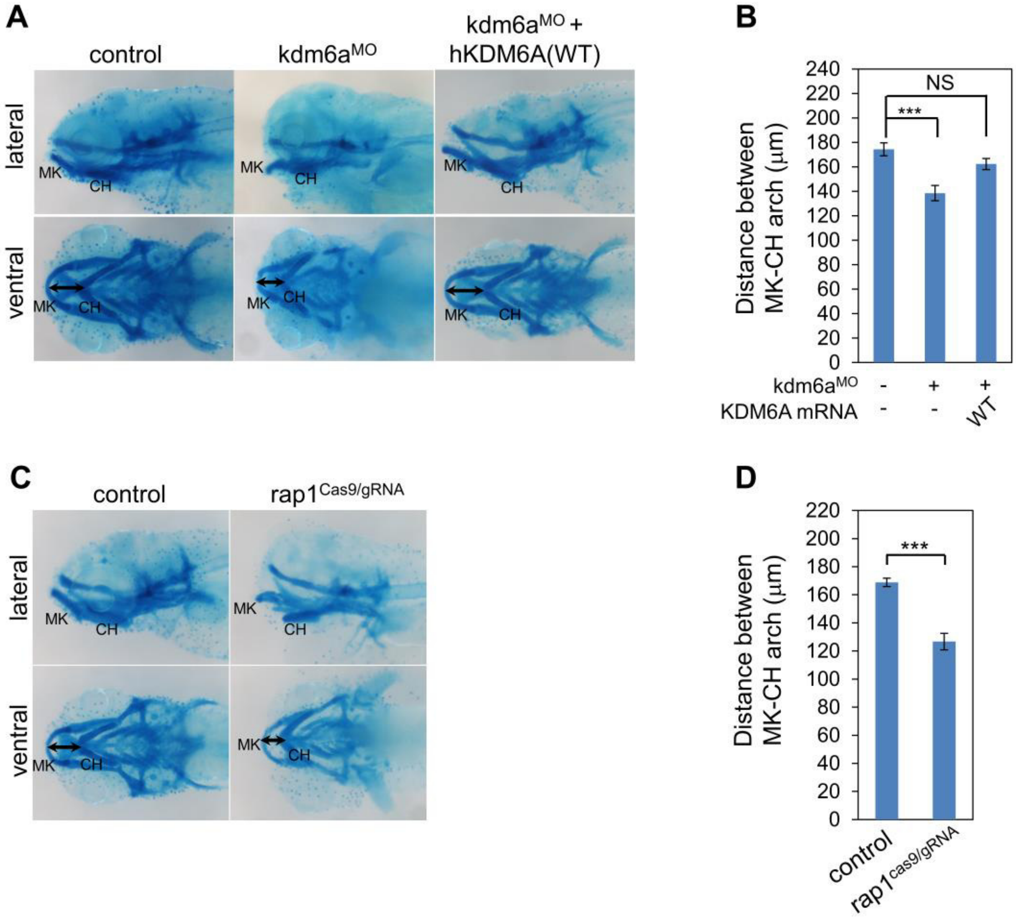

Supplementary Figure 3: Kabuki genes control proper jaw layout during early zebrafish development. A, Alcian blue staining of jaw cartilage. *Kdm6a* morphants have a lower ceratohyal (CH) arch (lateral view) and shorter distance between the Meckel (MK) and CH arch (ventral view; double arrow) in comparison to control embryos. The phenotype is rescued by human wild-type (wt) *KDM6A* mRNA. **B,** Quantitative measurement of the distance between MK and CH arch in *kmd6a* morphants (***: $p < 0.001$;). Statistical analysis using a 2-tailed Student's t-test ($n = 10$). **C,** Alcian blue staining of jaw cartilage. *Rap1*$^{\text{Cas9/gRNA}}$ embryos have lower ceratohyal (CH) arch (lateral view) and shorter distance between the MK and CH arch (ventral view; double arrow) in comparison to control embryos. **D,** Quantitative measurement of the distance between MK and CH shows the change in jaw layout of *rap1*$^{\text{Cas9/gRNA}}$ embryos (***: $p < 0.001$). Statistical analysis using a 2-tailed Student's t-test ($n > 30$). Error bars show s.e.m. (standard error of mean).

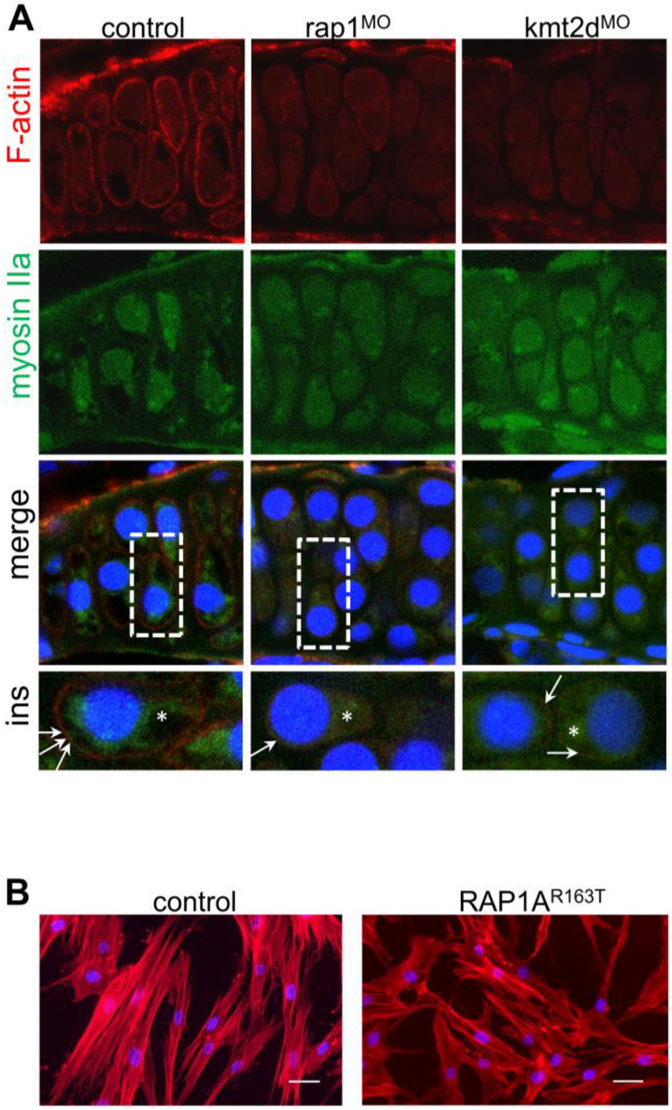

Supplementary Figure 4: Cytoskeleton alterations in *rap1* morphants and RAP1A^{R163T} fibroblasts. A, Phalloidin (red), myosin IIa (green) and DAPI (blue) staining in CH of 5 dpf zebrafish embryos. While chondrocytes in the control embryos line up and form well-organized actin filaments (F-actin), those in the *rap1* and *kmt2d* morphants are poorly arranged. F-actin and myosin IIa fail to polarize in the chondrocytes of *rap1* and *kmt2d* morphants. **B,** Phalloidin (red) and DAPI (blue) staining of RAP1A^{R163T} fibroblasts. Wild-type fibroblasts form a well-organized cell network. RAP1A^{R163T} fibroblasts exhibit disorganized cytoskeleton and cell-cell interaction. Scale bar represents 50 µm.

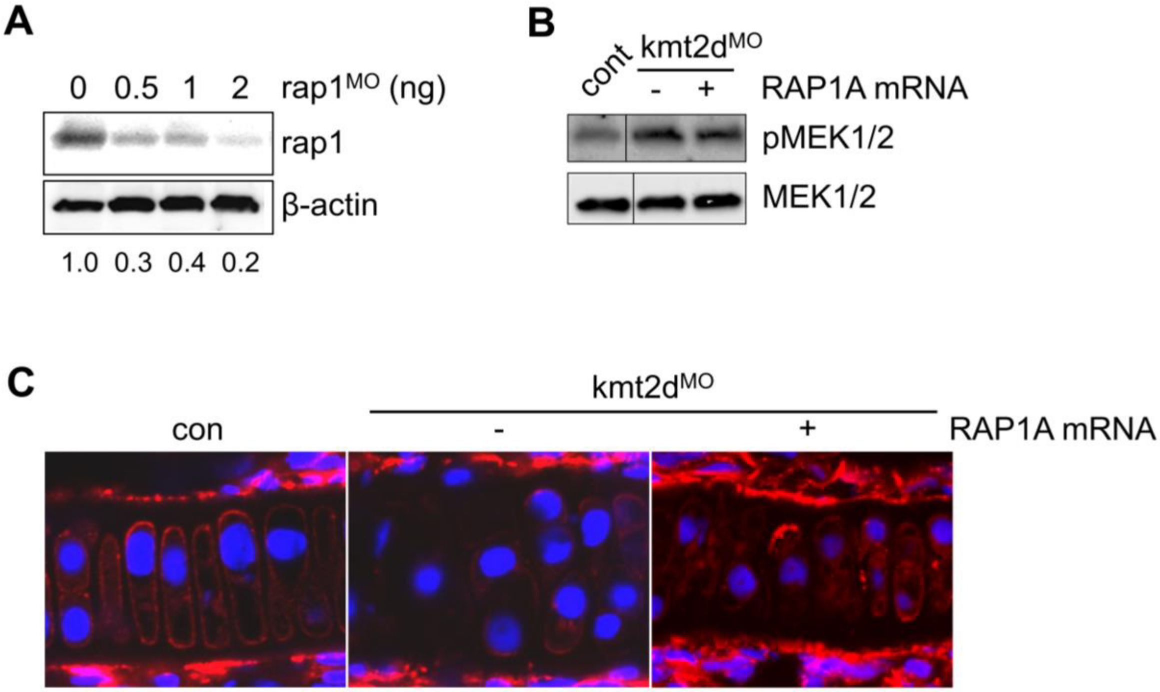

Supplementary Figure 5: Rap1 interacts genetically with kmt2d. A, Western blot analysis shows the knock-down efficiency of sub-effective doses of *rap1* morpholino. Relative levels of rap1 abundance are indicated at the bottom of blot. **B,** Expression of wild-type human *RAP1A* mRNA ameliorates the MAPK hyperactivation caused by loss of kmt2d. **C,** F-actin formation is inhibited in *kmt2d* morphant and can be rescued by expression of human *RAP1A*^{WT} mRNA.

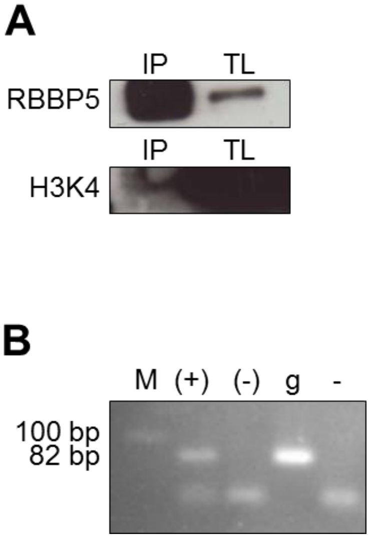

Supplementary Figure 6: The ASCOM complex can be found at the *RAP1B* promoter. A, ChIP experiments show that H3K4 can be detected from the immunoprecipitate of RBBP5 in wt human fibroblasts (IP, bottom), known to bind to KMT2D in the ASCOM complex. TL = total lysate. **B,** PCR analysis of a specific H3K4 trimethylated *RAP1B* promoter region (82 bp) in RBBP5-precipitated DNA of wt human fibroblasts. M = marker, (+) = IP with RBBP5 antibody, (-) = PCR negative control without antibody, g = PCR positive control, genomic DNA, - = PCR negative control without DNA.

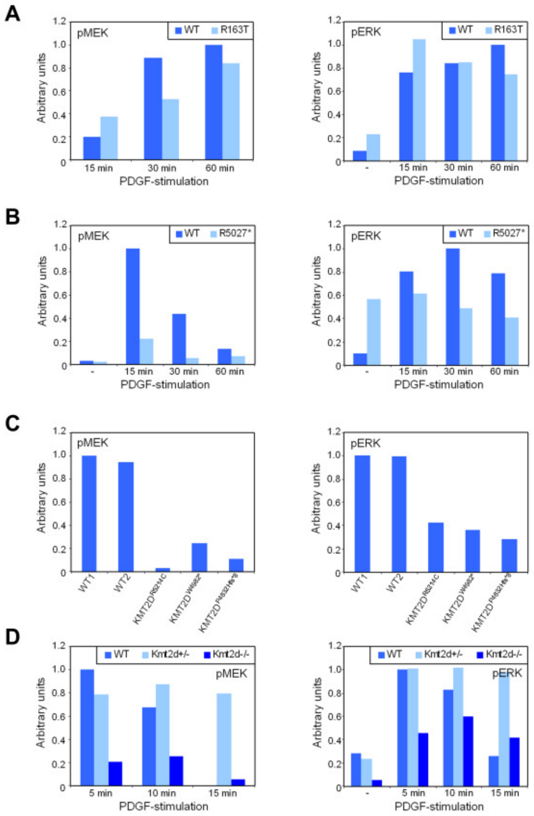

Supplementary Figure 7: Densitometric measurements of pMEK and pERK in patient cells and MEFs. A, Results of densitometric measurements of pMEK1/2 (left) and pERK1/2 (right) in fibroblasts from the index *RAP1A* patient normalized to total MEK1/2 and total ERK levels, respectively (corresponding to Western blot (WB) in Figure 8B). **B,** Results of densitometric measurements of pMEK (left) and pERK (right) in fibroblasts from a patient with KMT2D mutation p.R5027* normalized to total MEK and total ERK levels, respectively (corresponding to WB in Figure 8C). **C,** Results of densitometric measurements of pMEK (left) and pERK (right) in lymphoblastoid cell lines (LCLs) from 3 patients with different *KMT2D* mutations normalized to total MEK and total ERK levels, respectively (corresponding to WB in Figure 8D). **D,** Results of densitometric measurements of pMEK (left) and pERK (right) in mouse embryonic fibroblasts (MEFs) derived from *Kmt2d* knock-out mice normalized to total MEK and total ERK levels, respectively (corresponding to WB in Figure 8E).

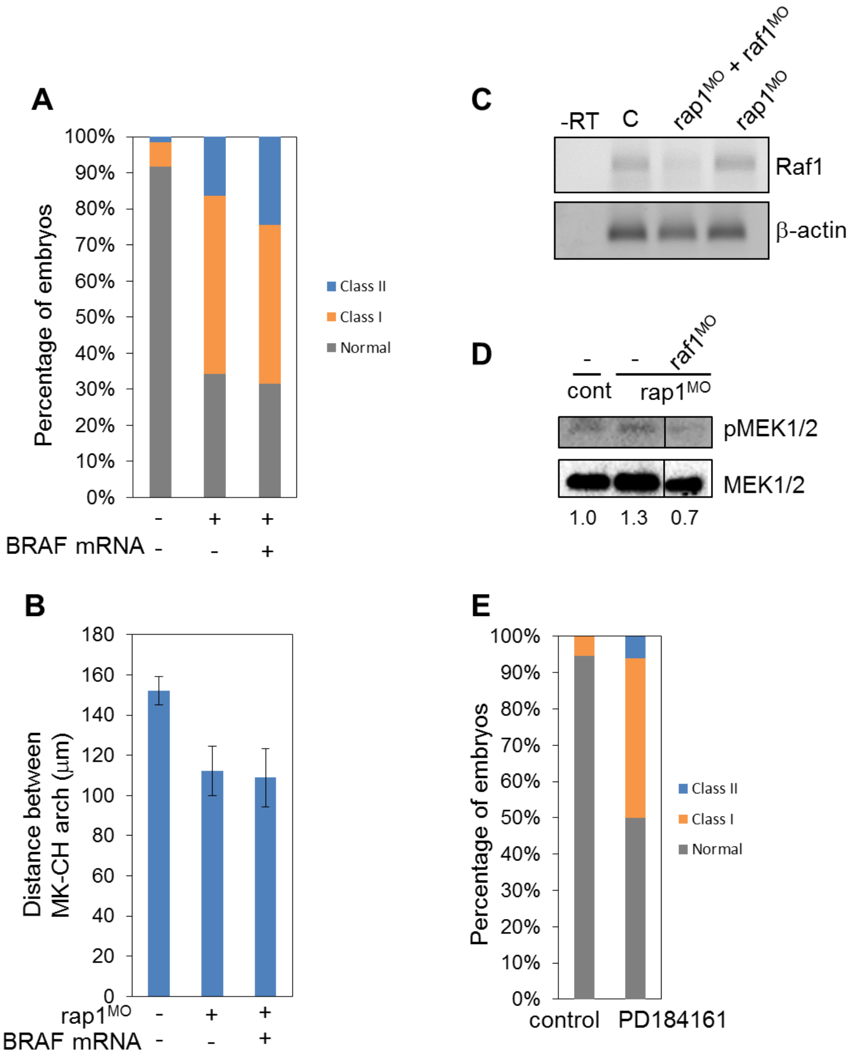

Supplementary Figure 8: Rap1-raf1-mediated MEK-ERK pathway is predominant in early zebrafish embryos. A, Expression of wild-type *BRAF* mRNA does not rescue the CE defects in *rap1* morphants. Statistical analysis using the chi-square test. **B,** Expression of wild-type *BRAF* mRNA does not rescue the jaw defects in *rap1* morphants. Statistical analysis using a 2-tailed Student's t-test (n = 10). **C,** RT-PCR for raf1 expression showed efficient knock-down of *raf1* by *raf1*^{MO1}. Knock-down of *rap1* does not affect the expression of raf1. C = control. **D,** Knock-down of *raf1* rescues MEK activation in the *rap1* morphant. Quantification of relative intensities indicated at the bottom. Experiment performed from a pool of 10 fish. **E,** Basal effect of MEK inhibitor PD184161 on CE movements. Statistical analysis using the chi-square test. Error bars show s.e.m.

Supplementary Table 1: Detected exome variants, *RAP1B* patient.

Filter	Remaining variations
Total	304238
Not in in-house database	63329
Not in dbSNP, 1000 Genomes or EVS	8380
Affecting protein sequence or splicing	322
De novo	1

Abbreviations: dbSNP = database of Single Nuclotide Polymorphisms, EVS = Exome Variant Server

Supplementary Table 2: Comparison of clinical signs of related syndromes.

Symptom	Kabuki	Noonan	Hadziselimovic
Short stature	+	+	+
Microcephaly	+	-	+
Neurological			
Intelectual disability	+	+	+
Developmental delay	+	+	+
Failure to thrive	+	+	+
Muscular hypotonia	+	-	+
Seizures / abnormal EEG	+	-	-
Hearing loss	+	+	-
Facial dysmorphism			
Long palpebral fissures	+	-	-
Downslanting palpebral fiss.	-	+	+
Eversion lat. lower eyelid	+	-	-
Long, dense eyelashes	+	-	-
Epicanthus	-	+	+
Arched eyebrows	+	-	-
Hypotelorism	-	-	+
Hypertelorism	-	+	-
Ptosis	+	+	+
Prominent ears	+	+	+
Low set ears	+	+	+
Cleft palate / high palate	+	+	+
Carp shaped mouth	+	-	+
Strabismus	+	-	+
Brain anomalies			
Corpus callosum anomalies	+	-	+
Cerebellar hypoplasia	-	-	+
Cerebral atrophy	+	-	-
Ventricular dilatation	+	-	-
White matter anomalies	+	-	-
Genitourinary anomalies			
Renal malformations	+	-	+
Cryptorchidism	+	+	-
Cong. heart defects	+	+	+
Skeletal findings			
Brachydactyly	+	+	-
Long digits	-	-	+
Hypoplastic digits	-	-	+
Asymmetric limb shortening	-	-	+
Chest anomalies	-	+	-
Scoliosis	+	+	-
Ectodermal			
Sparse hair	+	-	-
Whooly hair	-	+	-
Low anterior hairline	-	-	+
Low posterior hairline	-	+	-
Others			
Fetal finger pads	+	-	-
Frequent otitis	+	-	-
Webbed neck	-	+	-
Imperforate anus	+	-	+

Supplementary Table 3: Complete list of primer, morpholino, and CRISPR target sequences.

Primer name	**Primer sequence (5‘ – 3‘)**
PCR and sequencing for *RAP1A*	
RAP1A_E3F	GCCATGTAGCTTCTGTTGTCC
RAP1A_E3R	TCTGTGGTTATTAAATGATTTCCTG
RAP1A_E4F	CCATTAAGGGCAGAGGGC
RAP1A_E4R	TGTCCACATTAAGGAACAAGTCAC
RAP1A_E5F	GCATACTGCTGGAGACAGGC
RAP1A_E5R	TGAGCATGAACTACATCAGAGTTG
RAP1A_E5_F2	GACCGCTGTTCTTTATTGTG
RAP1A_E5_R2	CACACAGATTATTACAGGTGA
RAP1A_E6F	TTGCTAGAAACTTGTGTTATGTCTTG
RAP1A_E6R	GGCTCTTTCAGGCATGTGG
RAP1A_E7F	ATTTGATGAAGCTTGCGGTC
RAP1A_E7R	CCATCAAAGTGACCTTATGCAAG
RAP1A_E8F	TCAGCAGAGCCTTCTAACAAAC
RAP1A_E8R	GGAGAGGGCAAGTTATCCAAC
PCR and sequencing for *RAP1B*	
RAP1B_E2_F	GGTGCTCCATACTAGGGTTG
RAP1B_E2_R	TCCAGAGAGAATATGATCCACC
RAP1B_E3_F	CGAATGTAGTATTGGCTGTGG
RAP1B_E3_R	TGGTAACTATGCAATGCCAG
RAP1B_E4_F	GGTTTCCCTGTGTTGACTTG
RAP1B_E4_R	AAATTAAGGATTCAACGGAAC
RAP1B_E5_F	TTTGTATATAAATCGACTTTGGTG
RAP1B_E5_R	ACAGGATAATGGCAAAGGAG
RAP1B_E6_F	GAAGGCAGTGGAGATAATTGAC
RAP1B_E6_R	CTACATAGATACATTTAACATGAGGG
RAP1B_E7_F2	ATCTCTGCAGCTCCTTCAAC
RAP1B_E7_R2	TGATATTGCGCCACTGC
qPCR for *RAP1B* promoter (ChIP)	
RAP1B_1_F	GTTTAGGTGCAGGGTACAAACTT
RAP1B_1_R	GCCAAACGCAGTTAACAAATC
RAP1B_1-2_F	ATAAATGGCGTTGGTTTAGGTG
RAP1B_1-2_R	CAAATTCCCATGCCAAACG
RAP1B_2_F	TCTGAAAAACACTGATGTCTTTTG
RAP1B_2_R	ACCATCTGCTTTAACTTGCAAA
RAP1B_2-2_F	TTAAAACTACGCCCAGTGAACC
RAP1B_2-2_R	ATTAAAGAGAGTGGGAGAGGGG
qPCR for *HOXA7* promoter (ChIP)	
HOX7A_F	AGCCAGAACCCAAGACAGAG
HOX7A_R	GATTCTCCTCCCAGCCAAC
qPCR for *RAP1B* (Human)	
QuantiTect Primer Assay, Qiagen	
Hs_RAP1B_2_SG	QT01666560

qPCR for *BRAF* (Human)	
QuantiTect Primer Assay, Qiagen	
Hs_BRAF_1_SG	QT00078176
qPCR for *RAF1* (Human)	
QuantiTect Primer Assay, Qiagen	
Hs_RAF1_1_SG	QT00038969
qPCR for *Actin* (Human)	
QuantiTect Primer Assay, Qiagen	
Hs_ACTB_1_SG	QT00095431
Microsattelite marker analysis	
D1S180_F	CAT CGC TGA TTC GCA CAT TCCCTAAAAGACTGCAAGCT
D1S180_R	ACAGAGTCAAACTGTTGTGG
D1S187_F	CAT CGC TGA TTC GCA CAT AGGTGTGAGCTGTTCCCATA
D1S187_R	GCAAGACAGCTGCCTCATA
D1S200_F	CAT CGC TGA TTC GCA CATGTACTGTAACTTGGGTAACTGAAAC
D1S200_R	TGGCAGACCTGAACATCATA
D1S210_F	CAT CGC TGA TTC GCA CAT CCTCAGTTCATTCCCCATAA
D1S210_R	AGCTGAATCTCACCCAATAACTA
D1S217_F	CAT CGC TGA TTC GCA CAT TTATAACCAACCCTGTCACAG
D1S217_R	GCACATTTCCGGTAAAAGAA
D1S404_F	CAT CGC TGA TTC GCA CAT GGGACAAGTAGAAAGGGCA
D1S404_R	TGGAAGGTGGTAGAGGAAG
D1S466_F	CAT CGC TGA TTC GCA CAT CACTGCCTTTGGGGAC
D1S466_R	TCCTGCCTATCTGGGG
D1S1676_F	CAT CGC TGA TTC GCA CAT GGCACAGTTGGCAGAGTAAG
D1S1676_R	CTTGGACTGGAGCTTAGCCT
D1S1680_F	CAT CGC TGA TTC GCA CAT CTGTCCTGTGTGTGTCCTCA
D1S1680_R	GGGCTTTAAATGCTCTGACA
D1S2215_F	CAT CGC TGA TTC GCA CAT AGAGAGCCATTTACAATAGTC
D1S2215_R	ATTTGTCCATAATTAGCAACC
D1S2345_F	CAT CGC TGA TTC GCA CAT CAAGCTCCGTCTCAAAC
D1S2345_R	CATCTTCCCAATCTACAGG
D1S2346_F	CAT CGC TGA TTC GCA CAT TATCTTGCCCTGCACC
D1S2346_R	AAGTGGGTCTCCCCAG
D1S2612_F	CAT CGC TGA TTC GCA CAT GCTGTTCTTAGGGCTTTTCC
D1S2612_R	AACTTGGGCTTCTCTGCTTC
D1S2616_F	CAT CGC TGA TTC GCA CAT AGAGAGCAGATGGTGAGAC
D1S2616_R	ACTGAAATGAGAGCACATTG
D1S2640_F	CAT CGC TGA TTC GCA CAT TGTTGGAATGACCACCATA
D1S2640_R	ACTTAACACAATGGCCTGC
D1S2646_F	CAT CGC TGA TTC GCA CAT AGCTTAAATTGAGCAGGAAA
D1S2646_R	GGAGTAGATCATCACTGGGAG
D1S2652_F	CAT CGC TGA TTC GCA CAT GCAGGTGTGATGCCAGG
D1S2652_R	TACGGCTGATTGGGAGAAC
D1S2683_F	CAT CGC TGA TTC GCA CAT TGCCTTGTCTTCAAGAGC
D1S2683_R	GCAGTGACAGGAATCTGG
D1S2695_F	CAT CGC TGA TTC GCA CAT GGAGGGCACTGGCTACA

D1S2695_R	TGCTGGCTCAGGGGAC
D1S2726_F	CAT CGC TGA TTC GCA CAT CCACAAGTTGCAGGGTT
D1S2726_R	CTGGATGGATGCTCAAATAC
D1S2760_F	CAT CGC TGA TTC GCA CAT ACTGCACTCCAGCCTGGG
D1S2760_R	ATACGTTCTTACCTCAGGGGTTTCC
D1S2761_F	CAT CGC TGA TTC GCA CAT AAGACAGCTTTGCGTTTG
D1S2761_R	TGGCTGACCACAGGTAAT
D1S2795_F	CAT CGC TGA TTC GCA CAT TTAGTTGGATTAGACACGGC
D1S2795_R	GAGACCCTGATGACTGTGG
D1S2822_F	CAT CGC TGA TTC GCA CAT CAACTGCACTCTAACCTGG
D1S2822_R	AGTCTGACCCTGTACTGGTG
D1S2846_F	CAT CGC TGA TTC GCA CAT AGCTGTGCATAATGGGATTT
D1S2846_R	TTGGAAACTACAGGGTGCTT
D1S2855_F	CAT CGC TGA TTC GCA CAT GGAAATGGATGCAGAACTTG
D1S2855_R	AGCCTCTGGGCAGTGG
D1S2870_F	CAT CGC TGA TTC GCA CAT GATCATGCCAATGCACTAT
D1S2870_R	CCAGGGTGACACAGCA
D1S2885_F	CAT CGC TGA TTC GCA CAT GACATCCATCCCCTGGCTTA
D1S2885_R	GGGTCCCACTCGGGCT
D1S3466_F	CAT CGC TGA TTC GCA CAT ATGTCTTTGATCCTATGGAAGG
D1S3466_R	TGGGTAACAGACCCTGTCTC
qPCR in zebrafish	
zRaf1-F	GCTCCATCTCTACCTTCACTC
zRaf1-R	ACGTATGGCATCCTCAATCAG
zBraf-F	CCCAGAAACCCATCGTCAG
zBraf-R	TCTCCCCATCCTGAACTCTATAG
zRap1a-F	CTCGTCTACTCAATTACAGCTCAG
zRap1a-R	TTCCCCACAACTCTTTCATCC
zRap1b-F	TCCATAACAGCACAGTCCAC
zRap1b-R	TCCAGATCACACTTATTGCCC
zKmt2d-F	AGGAGAGCTTCAGTGTTTTGG
zKmt2d-R	GTTTATCAGCACCTCACCCTC
zActin-F	GAGAAGATCTGGCATCACACC
zActin-R	AGCTTCTCCTTGATGTCACG
Morpholinos	
rap1a	TGGTGGCAGATTATTTCTTTTCACC
rap1b	ACGCATTGTGCAGTGTGTCCGTTAA
kmt2d^{MO1}	AATCATTTATGTTTACTAACCTGCA
kmt2d^{MO2}	ATAGAAAGCCTTACAATGATGAGCT
kdm6a	GGAAACGGACTTTAACTGACCTGTC
raf1	AAAAAGCCTTCTCACAACTGTCCGC
CRISPR target sequences	
rap1a	GTGTTGGGCTCTGGTGGTGT
rap1b	TGCCAACACCTCCTGATCCG